

~~Central question  
d = 4 ?  
van der  
Waals  
competition  
16 D~~

## Chapter 2

### Pairing with transfer

#### 2.1 Nuclear Structure in a nutshell

The low-energy properties of the finite, quantal, many-body nuclear system, in which nucleons interact through the strong force of strength  $v_0 (\approx -100 \text{ MeV})$  and range  $a (\approx 1 \text{ fm})$  are controlled, in first approximation, by independent particle motion. This is a consequence of the fact that nucleons display a sizable value of the zero point (kinetic) energy of localization ( $\hbar^2/Ma \approx 40 \text{ MeV}$ ) as compared to the absolute value of the strength of the  $NN$ -potential  $|v_0| = 100 \text{ MeV}$

(App. 1.D).

The corresponding ground state  $|HF\rangle = \prod_i a_i^\dagger |0\rangle$  describes a step function in the probability of the occupied ( $\epsilon_i \leq \epsilon_F$ ) and empty ( $\epsilon_i > \epsilon_F$ ) states. Pushing the system it reacts with an inertia  $AM$ , sum of the nucleon masses. Setting it into rotation, assuming the density  $\rho(r) = \sum_i |\langle r|i \rangle|^2 (|i\rangle = a_i^\dagger |0\rangle)$  to be spatially deformed, it responds with the rigid moment of inertia. This is because the single-particle orbitals are solidly anchored to the mean field (Fig. 2.3, 3).

Pairing acting on nucleons moving in time reversal states  $v, \bar{v}$  ( $v \equiv (nlj)$ ), in configurations of the type  $((l)_{L=0}^2, (s)_{S=0}^2)$ , and lying close to the Fermi energy  $\epsilon_F (\approx 36 \text{ MeV})$ , alter this picture in a conspicuous way. Within an energy range of the order of the absolute value of the pair correlation energy  $E_{corr} (\approx -3 \text{ MeV})$ .

The corresponding ratio  $q = \left(\frac{\hbar^2}{Ma^2}\right) \frac{1}{|v_0|}$  is known as the quantity parameter and was first used in connection with the study of condensed matter (de Boer (1948, 1957); de Boer and Lundbeck (1948); Nosanow (1976)). It was introduced in nuclear physics in Mottelson (1998) where its value  $q = 0.4$  testifies to the validity of independent particle motion. It is noticeable that questions like the one posed in connection with localization and long mean free path were already discussed by Lindemann (1910) in connection with the study of the stability or less of crystals. The generalization to aperiodic crystals, like e.g. proteins (Schrödinger, E. (1944)) was carried out in Stillinger and Stillinger (1990). Its application to the atomic nucleus is discussed in App. 2.C.

Bogoliubov, R. A. and Zelevinsky, V. (2013).

<sup>3</sup>In BCS,  $E_{corr} \approx \frac{N(0)}{2} \Delta^2$ , where  $N(0) = \frac{g}{2}$  is the density of states at the Fermi energy and for one spin orientation,  $g_i = i/16 \text{ MeV}^{-1}$  ( $i = N, Z$ ) being the result of an empirical estimate which takes surface effects into account (Bohr, A. and Mottelson (1975); Bortignon, P. F. et al. (1998)), while  $\Delta$  is the pairing gap. For a typical superfluid, quadrupole deformed nucleus like  $^{170}\text{Yb}$ ,  $N(0) = 5.3 \text{ MeV}^{-1}$ ,  $\Delta \approx 1.1 \text{ MeV}$  and  $E_{corr} = -3.2 \text{ MeV}$  (Shimizu, Y. R. et al. (1989)).

Bohr, Mottelson and Pines (1958),

## normal (non-superfluid)

centered around  $\epsilon_F$  ( $|E_{corr}|/\epsilon_F \ll 1$ ), the role of independent particles is taken over by independent pairs of nucleons, correlated distances  $\xi \approx \hbar v_F/(2\Delta) (\approx 30 \text{ fm})$ , which flicker in and-out of the corresponding  $L = 0, S = 0$  configuration (Cooper pairs<sup>4,5</sup>).

For intrinsic<sup>6</sup> nuclear excitation energies and rotational frequencies<sup>7</sup> sensibly smaller than  $|E_{corr}/2|$  and  $\hbar\omega_{rot} \approx 0.5 \text{ MeV}$  respectively, the system can be described in terms of independent pair motion. This is a consequence of the fact that the kinetic energy of (Cooper) pair confinement ( $\hbar^2/(2M\xi^2) \approx 10^{-2} \text{ MeV}$ ), is much smaller than the absolute value of the pair binding energy  $|E_{corr}|$ , implying that each pair behaves as an entity<sup>8</sup> of mass  $2M$  and spin  $S = 0$ . Cooper pairs respect Bose-Einstein statistics, the single-particle orbits on which they correlate become dynamically detached from the mean field, leading to a bosonic-like condensate. This has a number of consequences. In particular, the moment of inertia  $I$  of quadrupole rotational bands of superfluid nuclei with open shells of both protons and neutrons is found to be smaller than the rigid moment of inertia by a factor of 2. The observed values, however, are a factor of 5 larger than the irrotational moment of inertia<sup>9</sup>, testifying to a subtle interplay between pairing and shear effects.

Cooper pairs exist also in situations in which the environmental conditions are above critical. For example, in metals at room temperature, in closed shell nuclei as well as in deformed open shell ones at high values of the angular momentum. However, in such circumstances, they break as soon as they are generated (pairing vibrations). While these pair addition and subtraction fluctuations have little effect in condensed matter systems with the exception that at<sup>10</sup>  $T \approx T_c$ , they play an important role in nuclei. In particular in nuclei around closed shells (Fig. 2.1.1), and specially in the case of light, highly polarizable, exotic halo nuclei<sup>11</sup>. From this vantage point one can posit that it is not so much, or, at least not only, the superfluid

<sup>4</sup>Cooper (1956).

<sup>5</sup>Brink, D. and Broglia (2005).

<sup>6</sup>As opposed to collective excitations, excitations which do not alter the temperature of the system.

<sup>7</sup>Coriolis force acts oppositely on each member of a Cooper pair. When the difference in rotational energy between superfluid and normal rotation becomes about equal to the correlation energy, the nucleon moving opposite to the collective rotation becomes so much retarded in its revolution period with respect to the partner nucleon, that eventually it cannot correlate any more with it and “align” its motion (and spin) with the rotational motion, becoming again a pair of fermions and not participating any more in the condensate. This happens for a (critical) angular momentum  $I_c \approx (120 \times |E_{corr}|)^{1/2} \approx 20\hbar$ , corresponding to a rotational frequency  $\hbar\omega_c \approx 0.5 \text{ MeV}$  (Brink, D. and Broglia (2005)).

<sup>8</sup>The ratio  $q\xi = \frac{\hbar^2}{2M\xi^2} \frac{1}{|E_{corr}|} \approx 0.007$  provides a generalized quantity parameter. It testifies to the stability of nuclear Cooper pairs in superfluid nuclei.

<sup>9</sup>Bohr, A. and Mottelson (1975); Belyaev (1959); Belyaev, S. T. (2013).

<sup>10</sup>Schmid, A. (1966), Schmidt, H. (1968), Schmid, A. (1969) Abrahams, E. and Woo (1968); concerning superfluid  ${}^3\text{He}$  cf. Wölfe, P. (1978).

<sup>11</sup>See Sects. 2.5 and 2.6; Bohr, A. and Mottelson (1975), Bès, D. R. and Broglia (1966), Högaasen-Feldman (1961), Schmidt, H. (1972), Schmidt, H. (1968), Barranco, F. et al. (2001), Potel, G. et al. (2013a), Potel et al. (2014).

*state* which is abnormal in the nuclear case, but the normal state associated with closed shell systems<sup>12</sup>. It is of notice nonetheless, the role pairing vibrations play in the transition between superfluid and normal nuclear phases (cf. Fig. 2.1.2) as a function of the rotational frequency (angular momentum) as emerged from the experimental studies of high spin states carried out by, among others, Garrett and collaborators<sup>13</sup>.

From Fig. 2.1.2 it is seen that while the dynamic pairing gap associated with pairing vibrations leads to a  $\approx 20\%$  increase of the static pairing gap for low rotational frequencies, it becomes the overwhelming contribution above the critical frequency<sup>14</sup>. In any case, the central role played by pairing vibrations within the present circumstances is that to restore particle-number conservation, another example after that provided by the quantity parameter and by its generalization to pair motion, of the fact that potential functionals are, as a rule, best profited by special arrangements of fermions (spontaneous symmetry breaking), while fluctuations ~~restore~~ symmetry<sup>15</sup>.

Within this context, there are a number of methods which allows one to go beyond mean-field approximation (HFB). Generally referred to as number projection methods<sup>16</sup>(NP), they make use of a variety of techniques (Generator Coordinate Method, Pfaffians, etc.) as well as protocols (variation after projection, gradient method, etc.). The advantages of NP methods over the RPA is to lead to smooth functions for both the correlation energy and the pairing gap at the pairing phase transition between normal and superfluid phases. That is, between the pairing vibrational and pairing rotational schemes<sup>17</sup>.

The above results underscore the fact that, at the basis of an operative coarse grained approximation to the nuclear many-body problem (within this context cf. App. 1.D, in particular the discussion following Eq. 1.D.5), one finds a judicious choice of the collective coordinates<sup>18</sup>. In other words, pairing vibrations are elementary modes of excitation containing the right physics to restore gauge invariance through their interweaving with quasiparticle states. Within the framework of the above picture, one can introduce at profit a collective coordinate  $\alpha_0$  (order parameter) which measures the number of Cooper pairs participating in the pairing condensate, and define a wavefunction for each pair  $(U'_v + V'_v a'_v a'^{\dagger}_v)|0\rangle$  (independ-

<sup>12</sup> See Potel, G. et al. (2013a) and refs. therein. Also Potel, G. et al. (2013b) in connection with the closed shell system  $^{132}\text{Sn}$ .

<sup>13</sup> cf. Shimizu, Y. R. et al. (1989); <sup>see</sup> also Brink, D. and Broglia (2005), Ch. 6 and references therein.

<sup>14</sup> Shimizu, Y. R. et al. (1989), Shimizu, Y. R. and Broglia (1990), Shimizu, Y. R. (2013), Dönau, F. et al. (1999) Shimizu, Y. R. et al. (2000).

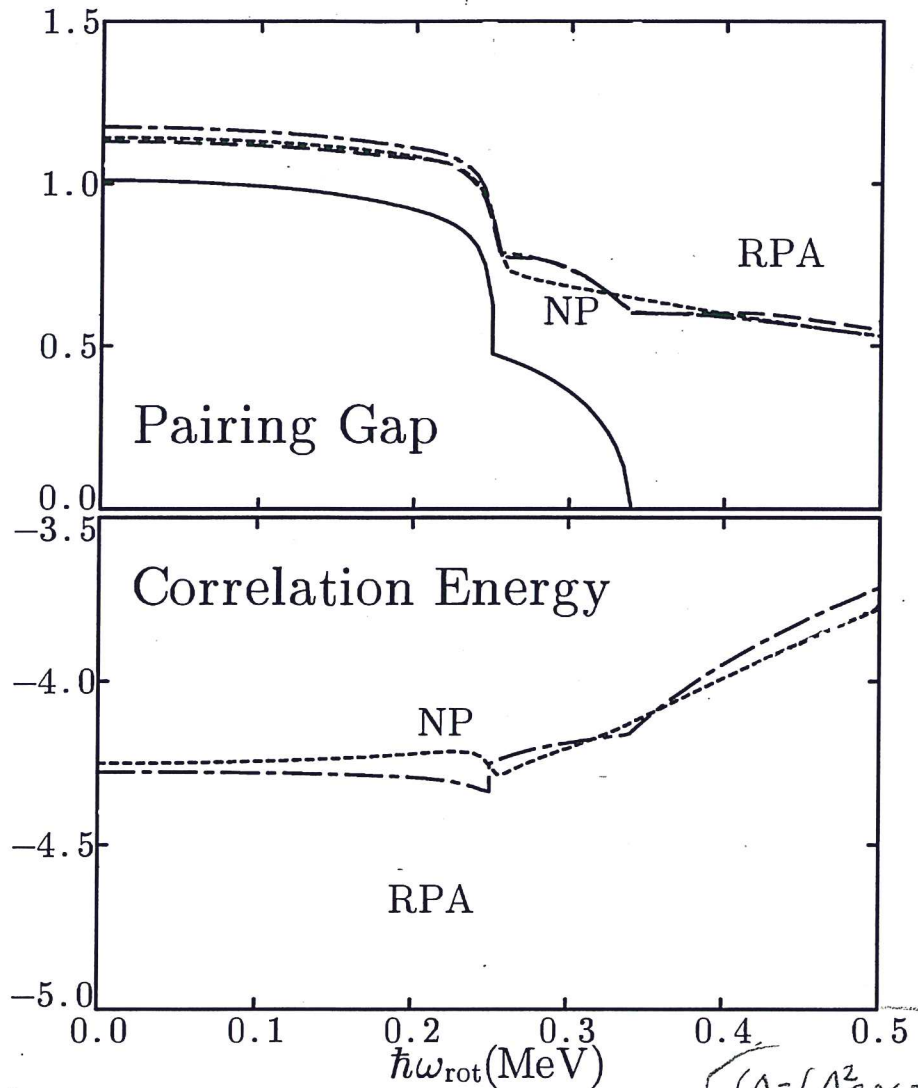
<sup>15</sup> Andersson and Stein (1984); Aderson (1976).

<sup>16</sup> cf. Ring, P. and Schuck (1980), Egido, J. L. (2013), Robledo, R. M. and Bertsch (2013); cf. also Frauendorf, S. (2013), Ring, P. (2013), Heenen, P. H. et al. (2013), and references therein.

<sup>17</sup> Figs. 2.1.1, 2.1.3, 2.1.4, see also Fig. 2.4.1 and Sects. 2.4.2 and 2.5; cf. Bès, D. R. and Broglia (1966), Bohr, A. and Mottelson (1975) and references therein.

<sup>18</sup> In this connection, we quote allegedly from S. Weinberg: "In solving a problem you may choose to use the degrees of freedom you like. But if you choose the wrong ones you will be sorry".

\* ) See e.g. Bès and Broglia (1971a), (1971b), ~~(1971c)~~  
• (1971c)



V  
Figure 2.1.2: Pairing gap calculated taking into account the correlation associated with pair vibrations in the RPA approximation ( $\Delta = (\Delta_{BCS}^2 + \frac{1}{2}G^2 S_0(RPA))^{1/2}$ ) (upper panel) and RPA correlation energy (lower panel) for neutrons in  $^{164}\text{Er}$  as a function of the rotational frequency. Both quantities are in MeV (dashed-dotted curves). The value of the static (mean-field) pairing gap  $\Delta$ , which vanishes at  $\hbar\omega_{\text{rot}} = 0.34$  MeV, is also displayed in the upper panel (continuous curve). The results of the number-projection (NP) calculations are shown as dotted curves.  $S_0(RPA) = \sum_{n \neq AGN} [ < n|P|0 > + < n|P^\dagger|0 > ]^2_{RPA}$ , where  $\Delta_{BCS} = G < BCS|P^\dagger|BCS >$  is the standard, static BCS pairing gap, while  $G$  is the pairing force strength. The non-energy weighted sum rule  $S_0(RPA)$  describes the contribution of pairing fluctuations to the effective (RPA) gap, and is intimately associated with projection in particle number. It is of notice that  $\sum_{n \neq AGN}$  means that the divergent contribution from the zero energy mode (Anderson, Goldstone, Nambu mode, see e.g. Broglia et al. (2000) and references therein), associated with the lowest ( $\hbar\omega_0$ ) solution of the  $H = H'_p + H''_p$  (cf. Sect 6.2.3 and Brink, D. and Broglia (2005) App. J) is to be excluded (after Shimizu, Y. R. and Broglia (1990)).

$$(\Delta = (\Delta_{BCS}^2 + \frac{1}{2}G^2 S_0(RPA))^{1/2})$$

(Brink D. and Broglia (2005)  
Sect. 6.6)

~~explain  $U'_v$   $V'_v$  pairs~~

dent pair motion, BCS approximation, cf. Figs. 2.4.1, 2.4.2 and 2.4.3), adjusting the occupation parameters  $V_v$  and  $U_v$  (probability amplitudes that the two-fold, Kramer's-degenerate pair state  $(v, \bar{v})$ , is either occupied or empty), so as to minimize the energy of the system under the condition that the average number of nucleons is equal to  $N_0$  (the Coriolis-like force felt, in the intrinsic system in gauge space by the Cooper pairs, being equal to  $-\lambda N_0$ ). Thus,  $|BCS\rangle = \prod_{v>0} (U'_v + V'_v a'_v a'^{\dagger}_v) |0\rangle$  provides a valid description of the independent pair mean field ground state, and of the associated order parameter  $\alpha'_0 = \langle BCS | P'^{\dagger} | BCS \rangle = \sum_{v>0} U'_v V'_v$ ,  $P'^{\dagger} = \sum_{v>0} a'^{\dagger}_v a'^{\dagger}_v$  being the pair creation operator<sup>19</sup>. It is then natural to posit that two-particle transfer reactions are specific to probe pairing correlations in many-body fermionic systems. Examples are provided by the Josephson effect<sup>20</sup> between e.g. metallic superconductors, and  $(t, p)$  and  $(p, t)$  reactions in atomic nuclei<sup>21</sup>.

stop

Within this context we now take the basic consequence of pairing condensation in nuclei regarding reaction mechanisms. For this purpose let us consider a *gedanken experiment* in which the superfluid target and the projectile can at best come in such weak contact that only single-nucleon transfer leads to a yield falling within the sensitivity range of the measuring setup. Because  $(\hbar^2/2M\xi^2)/|E_{corr}| \approx 10^{-2}$ , Cooper pairs in superfluid nuclei behave as particles of mass  $2M$  over distances  $\xi$ , even in the case in which the  $NN$ -potential vanishes in the zone between the weakly overlapping densities of the two interacting nuclei. One then expects Cooper pair transfer to be observed. Not only. One also expects that the associated absolute differential cross section contains, for the particular choice of mass number  $d$  and within the framework of the theory of quantum measurement, all the information needed to work out a comprehensive description of nuclear superfluidity.

made

Because  $\alpha_0 \sim N(0)$ , cross sections associated with the transfer of Cooper pairs between members of a pairing rotational band, are proportional to the density of single-particle levels quantity squared. As a consequence, absolute two-nucleon transfer cross sections are expected to be of the same order of magnitude than one-nucleon transfer ones, and to be dominated by successive transfer. These expectations have been confirmed experimentally and by detailed numerical calculations, respectively. The above parlance, being at the basis of the Josephson effect, reflects both one of the most solidly established results in the study of BCS pairing, and explains the workings of a paradigmatic probe of spontaneous symmetry breaking phenomena.

Due to the fact that, away from the Fermi energy pair motion becomes independent particle motion (see Sect. 2.4), one-particle transfer reactions like e.g.  $(d, p)$  and  $(p, d)$  can be used together with  $(t, p)$  and  $(p, t)$  processes, as valid tools

<sup>19</sup>cf. Bardeen et al. (1957a), Bardeen et al. (1957b), Schrieffer (1964), Schrieffer, J. R. (1973) and references therein.

<sup>20</sup>Josephson (1962).

<sup>21</sup>cf. e.g. Yoshida (1962), Broglia, R.A. et al. (1973), Bayman (1971), Glendenning, N. K. (1965), Bohr (1964), Hansen (2013) and Potel, G. et al. (2013a) and references therein; cf. also Figs. 2.1.1, 2.1.3 and 2.1.4.

*physical shell  
rule*

## 2.1. NUCLEAR STRUCTURE IN A NUTSHELL

121

to cross check pair correlation predictions (see Chapter 4). In particular, to shed light on the origin of pairing in nuclei: in a nutshell, the relative importance of the bare  $NN$ -interaction and the induced pairing interaction (within this context see Sect. 2.6).

While the calculation of two-nucleon transfer spectroscopic amplitudes and differential cross sections are, a priori, more involved to be worked out than those associated with one-nucleon transfer reactions, the former are, as a rule, more “intrinsically” accurate than the latter ones. This is because, in the case of two nucleon transfer reactions, the quantity (order parameter  $\alpha'_0$ ) which expresses the collectivity of the members of a pairing rotational band, reflects the properties of a coherent state ( $|BCS\rangle$ ). In other words, it results from the sum over many contributions ( $\sqrt{j_\nu + 1/2} U'_\nu V'_\nu$ , cf. Sect. 2.4), all of them having the same phase. Consequently, the relative error decreases as the square root of the number contributions ( $\approx N(0)\Delta \approx 4 \text{ MeV}^{-1} \times 1.4 \text{ MeV} \approx 6$  in the case of the superfluid nucleus  $^{120}\text{Sn}$ ).

There is a further reason which confers  $\alpha'_0 = \sum_j (j + 1/2) U'_j V'_j$  a privileged position with respect to the single contributions  $(j + 1/2) U'_j V'_j$ . It is the fact that  $\alpha'_0 = e^{2i\varphi} \sum_j (j + 1/2) U_j V_j = e^{2i\varphi} \alpha_0$  defines a privileged orientation in gauge space,  $\alpha_0$  being the order parameter referred to the laboratory system which makes an angle  $\varphi$  in gauge space with respect to the intrinsic system to which  $\alpha'_0$  is referred.<sup>(2)</sup> In other words, the quantities  $\alpha'_0$  which measure the deformation of the superfluid nuclear system in gauge space, and the rotational frequency  $\lambda = \hbar\dot{\varphi}$  in this space, and associated Coriolis force  $-\lambda N_0$  felt by the nucleons referred to the body fixed frame, are the result of solving selfconsistently the BCS number

and gap equations  $N_0 = \sum_j (2j + 1) \left( 1 - \frac{(\epsilon_j - \lambda)/\Delta}{\sqrt{1 + (\frac{\epsilon_j - \lambda}{\Delta})^2}} \right)$  and  $\alpha'_0 = \sum_j (j + 1/2) U'_j V'_j = \sum_j (j + 1/2) \left( 1 - 1/\sqrt{1 + (\frac{\epsilon_j - \lambda}{\Delta})^2} \right)$  making use as inputs  $\epsilon_\nu$ ,  $N_0$  and  $\Delta$ , that is single-particle energies, the average number of particles and the pairing gap.

Similar arguments can be used regarding the excitation of pairing vibrations in terms of Cooper pair transfer from closed shells as compared to one-particle transfer. As seen from Fig. 2.1.5 (b)-(c), the random phase approximation (RPA) amplitudes  $X_\nu^a$  and  $Y_\nu^a$  sum coherently over pairs of time reversal states,<sup>\*</sup> to give rise to the spectroscopic amplitudes associated with the direct excitation of the pair addition mode displayed in (d). Because of the (dispersion) relation (b)+(c) $\equiv$ (d), the  $X_\nu$ - and  $Y_\nu$ -amplitudes are correlated, among themselves as well as in phase. As seen from (g) and (h), the situation is quite different in the case of one-particle transfer. The soundness of the above parlance reflects itself in the calculation of the elements resulting from the encounter of structure and reaction, namely one- and two-nucleon modified transfer formfactors. While it is usually considered that these quantities carry all the structure information associated with the calculation

<sup>(2)</sup> See Sect. 2.4.2, see Potel, G. et al. (2013b).

\* ) Brink, D. and Broglia (2005) ch. 5 .

*written  
answer to  
Bogusmans  
comment*

*U upper  
case*

*U' V'*

where

$$\begin{aligned} \Psi_{M_f}^{J_f}(\xi_{A+2}) &= \sum_{\substack{n_1 l_1 j_1 \\ n_2 l_2 j_2 \\ J, J'_i}} B(n_1 l_1 j_1, n_2 l_2 j_2; J J'_i J_f) \\ &\quad \times [\phi^J(n_1 l_1 j_1, n_2 l_2 j_2) \Psi_{M_i}^{J'_i}(\xi_A)]_{M_f}^{J_f}, \end{aligned} \quad (2.1.5)$$

and

$$\Psi_{\text{entrance}} = \Psi_{M_i}^{J_i}(\xi_A) \times \phi_t(\mathbf{r}_{n1}, \mathbf{r}_{n2}, r_p; \sigma_{n1}, \sigma_{n2}, \sigma_p), \quad (2.1.6)$$

with

$$\phi_t = [\chi^S(\sigma_{n1}, \sigma_{n2}) \chi^{S'_f}(\sigma_p)]_{M_{S_i}}^{S_i} \times \phi_t^{L=0} \left( \sum_{i>j} |\mathbf{r}_i - \mathbf{r}_j| \right). \quad (2.1.7)$$

Assuming for simplicity a symmetric di-neutron radial wavefunction for the triton (i.e. neglecting the  $d$ -component of the corresponding wavefunction) both for the relative and for the center of mass wavefunctions  $\phi_{nlm}(\mathbf{r})$  and  $\phi_{N\Lambda M}(R)$  ( $n = l = m = 0, N = \Lambda = M = 0$ ), leads to  $\Omega_n$ , a quantity which reflects both the non-orthogonality existing between the di-neutron wavefunctions in the final nucleus (Cooper pair) and in the triton as well as their degree of  $s$ -wave of relative motion. Another way to say the same thing is to state that dineutron correlations in these two systems are different, a fact which underscores the limitations of light ion reactions to probe specifically pairing correlations in nuclei<sup>(26)</sup>.

One can then conclude that, provided one makes use of a (sensible) complete single-particle basis (eventually including also the continuum), one can capture through  $u_{LSJ}^{J_f}(R)$  most of the coherence of Cooper pair transfer, as a major fraction of the associated di-neutron non-locality is taken care of by the  $n$ -summation appearing in eq. (2.1.1), the different contributions being weighted by the non-orthogonality overlaps  $\Omega_n$ . This is in keeping with the fact that, making use of a more refined triton wavefunction than that employed above, the  $n - p$  (deuteron-like) correlations of this particle can be described with reasonable accuracy and thus, the emergence of successive transfer (see Chapter 3). On the other hand, being the deuteron a bound system, this effective treatment of the associated resonances is not particularly economic. Furthermore, it is of notice that the zero-range approximation ( $V(\rho)\phi_{000}(\rho) = D_0\delta(\vec{\rho})$ ) eliminates the above mentioned possibilities (cf. eq. (5.B.19))

Anyhow, the fact that one can still work out a detailed and physically insightful picture of two-nucleon transfer reactions in nuclei in terms of absolute cross sections with the help of a single parameter ( $D_0^2 \approx (31.6 \pm 9.3)10^4 \text{ MeV}^2 \text{ fm}^2$ ) testifies to the fact that the above picture of Cooper pair transfer<sup>(27)</sup> is a useful one, as it contains a large fraction of the physics which is at the basis of Cooper pair transfer in nuclei<sup>(28)</sup>. This is in keeping with the fact that the Cooper pair correlation length

<sup>(26)</sup> Within this context see von Oertzen and Vitturi (2001), von Oertzen, W. (2013).

<sup>(27)</sup> Glendenning, N. K. (1965), Bayman and Kallio (1967).

<sup>(28)</sup> Broglia, R.A. et al. (1973).

is much larger than nuclear dimensions and, consequently, simultaneous and successive transfer feel the same pairing correlations (see Chapter 3). In other words, treating explicitly the intermediate deuteron channel in terms of successive transfer, correcting both this and the simultaneous transfer channels for non-orthogonality contributions, makes the above picture the quantitative probe of Cooper pair correlations in nuclei<sup>29</sup> (Fig. 2.2.1).

Within the above context, we provide below two examples of  $B$ -coefficients associated with coherent states. Namely, one for the case in which  $A$  and  $B (= A+2)$  are members of a pairing rotational band. A second one, in the case in which they are members of a pairing vibrational band. That is,

$$1), B(nlj, nlj; 000) = \langle BCS(N+2) | \frac{[a_{nlj}^\dagger a_{nlj}^0]^0}{\sqrt{2}} | BCS(N) \rangle \\ = \sqrt{j+1/2} U_{nlj}(N) V_{nlj}(N+2), \quad (2.1.8)$$

and

$$2), B(nlj, nlj; 000) = \langle (N_0 + 2)(gs) | \frac{[a_{nlj}^\dagger a_{nlj}^0]^0}{\sqrt{2}} | N_0(gs) \rangle \\ = \begin{cases} \sqrt{j_k + 1/2} X^a(n_k l_k j_k) & (\epsilon_{j_k} > \epsilon_F) \\ \sqrt{j_k + 1/2} Y^a(n_i l_i j_i) & (\epsilon_{j_k} \leq \epsilon_F). \end{cases} \quad (2.1.9)$$

Where the  $X$  and  $Y$  coefficients are the forwardgoing and backwardgoing RPA amplitudes of the pair addition mode.\* For actual numerical values see Sect. 2.4, Table 2.4.1 and Sect. 2.5 Tables 2.5.2–2.5.5.

We conclude this section by remarking that, in spite of the fact that one is dealing with the connection between structure and direct transfer reactions, no mention has been made of spectroscopic factors in relation with one-particle transfer processes, let alone when discussing two-particle transfer. In fact, one will be using throughout the present monograph, exception made when explicitly mentioned, absolute cross sections as the sole link between spectroscopic amplitudes and experimental observations.

## 2.2 Renormalization and spectroscopic amplitudes

Elementary modes of nuclear excitation, namely single-particle motion, vibrations and rotations, being tailored to economically describe the nuclear response to external probes, contain a large fraction of the many-body correlations. Consequently, their wavefunctions are non-orthogonal to each other, in keeping with the fact that all the degrees of freedom of the nucleus are exhausted by those of the nucleons

<sup>29</sup> Bayman and Chen (1982) and Potel, G. et al. (2013a).

\* Brink, D. and Broglia (2005), ch. 5.

(see Chapter 1). The corresponding overlaps give a measure of the strength with which the different modes couple to each other. The resulting particle-vibration coupling Hamiltonian can be diagonalized, making use of Nuclear Field Theory<sup>10</sup>, and of the BRST techniques<sup>(31)</sup> in the case of particle-rotor coupling.

As a result of the interweaving of single-particle and collective motion, the nucleons acquire a state dependent self energy  $\Delta E_j(\omega)$  which, for levels far away from the Fermi energy can become complex. Consequently, the single-particle potential which was already non-local in space (exchange potential, related to the Pauli principle) becomes also non-local in time (retardation effects; cf. e.g. Fig. 2.6.3 (I)). There are a number of techniques to make it local. In particular the Local Density Approximation (LDA) and the effective mass approximation. In this last case one can describe the single-particle motion in terms of a local (complex) potential with a real part given by  $U'(r) = (m/m^*)U(r)$ , where  $m^* = m_k m_\omega / m$  is the effective nucleon mass,  $m_k$  being the so-called  $k$ -mass (non-locality in space in keeping with the fact that  $\Delta x \Delta k_x \geq 1$ ), and  $m_\omega = m(1 + \lambda)$  being the  $\omega$ -mass (non-locality in time, as implied by the relation  $\Delta \omega \Delta t \geq 1$ ),  $\lambda = -\partial \Delta E(\omega) / \partial \hbar \omega$  being the so-called mass enhancement factor. It reflects the ability with which vibrations cloth single-particles. In other words, it measures the probability with which a nucleon moving at  $t = -\infty$  in a "pure" orbital  $j$  can be found at a later time in a  $2p - 1h$  like (doorway state)  $|j'L; j\rangle$ ,  $L$  being the multipolarity of a vibrational state. Within this context, the discontinuity taking place at the Fermi energy in the dressed particle picture ( $Z_\omega = (m/m_\omega)^{1/2}$ , cf. Appendix D introducción) is connected with the single-particle occupancy probability<sup>(\*)</sup>.

It is of notice that dressed particles automatically imply an induced pairing interaction (see e.g. Figs. 2.6.3 (I) and (II)) resulting from the exchange of the clothing vibrations between pairs of nucleons moving in time reversal states close to the Fermi energy. In other words, fluctuations in the normal density ( $\delta \rho$ , cf. Fig. 4.A.1 (i)) and the associated particle-vibration coupling vertices lead to abnormal (superfluid) density (deformation in gauge space). Whether this is a dynamic or static effect, depends on whether the parameter (cf. Fig. 2.5.7) <sup>\*\*</sup>)

$$x' = G' N'(0), \quad (2.2.1)$$

product of the effective pairing strength,

$$G' = Z_\omega^2 (v_p^{bare} + v_p^{ind}), \quad (2.2.2)$$

and of the renormalized density of levels  $N'(0)$  is considerable smaller (larger) than  $\approx 1/2$ . The quantity  $G'$  is the sum of the bare and induced pairing interaction, renormalized by the degree of single-particle content of the levels where nucleons correlate. The quantity

$$N'(0) = Z_\omega^{-1} N(0) = (1 + \lambda) N(0) \quad (2.2.3)$$

<sup>10</sup>NFT, cf. Bortignon, P. F. et al. (1977), Bortignon, P. F. et al. (1978).  
<sup>31</sup>cf. Bès, D. R. and Kurchan (1990).

<sup>\*\*</sup>) Brühn D. and Broglie R. A (2005) Ch. 9.  
<sup>\*\*</sup>) Brühn D. and Broglie R. A (2005) App. H  
Sect. H.4; Barranco et al (2005)

is the similarly renormalized density of levels at the Fermi energy. From the above relations one obtains

$$x' = Z_\omega(v_p^{bare} + v_p^{ind})N(0). \quad (2.2.4)$$

All of the above many-body,  $\omega$ -dependent effects which imply in many cases a coherent sum of amplitudes, are not simple to capture in a spectroscopic factor in connection with one-particle transfer, let alone two-nucleon transfer processes<sup>32</sup>.

In keeping with the fact that  $m_k \approx 0.6 - 0.7m$  and that  $m^* \approx m$ , as testified by the satisfactory fitting standard Saxon-Woods potentials provides for the valence orbitals of nucleons of mass  $m$  around closed shells, one obtains  $m_\omega \approx 1.4 - 1.7m$ . Thus  $Z_\omega \approx 0.6 - 0.7$ . It is still an open question how much of the observed single-particle depopulation can be due to hard core effects, which shifts the associated strength to high momentum levels<sup>33</sup>. An estimate of such an effect of about 20% will not quantitative change the long wavelength estimate of  $Z_\omega$  given above. Arguably, a much larger depopulation through hard core effects remains an open problem within the overall picture of elementary modes of nuclear excitation and of medium polarization effects.

### 2.3 Quantality Parameter

The quantality parameter<sup>34</sup> is defined as the ratio of the quantal kinetic energy of localization and potential energy, (cf. Fig. 2.3.1 and Table 2.3.1). Fluctuations, quantal or classical, favor symmetry: gases and liquids are homogeneous. Potential energy on the other hand prefers special arrangements: atoms like to be at specific distances and orientations from each other (spontaneous breaking of translational and of rotational symmetry reflecting the homogeneity and isotropy of empty space<sup>35</sup>).

When  $q$  is small, quantal effects are small and the lower state for  $T < T_c$  will have a crystalline structure,  $T_c$  denoting the critical temperature. For sufficiently large values of  $q (> 0.15)$  the system will display particle delocalization and, likely, be amenable, within some approximation, to a mean field description (Figs. 2.3.2

<sup>32</sup>See Barranco et al. (2005), Barranco et al (1999) ↵

<sup>33</sup>Cf. Dickhoff, W. and Van Neck (2005), Jenning, B. (2011), Kramer, G. J. et al. (2001), Barbieri, C. (2009), Schiffer, J. P. et al. (2012), Duguet, T. and Hagen (2012), Furnstahl, R. J. and Schwenk (2010).

<sup>34</sup>Nosanow (1976), de Boer (1957), de Boer (1948), de Boer and Lundbeck (1948), Mottelson (1998).

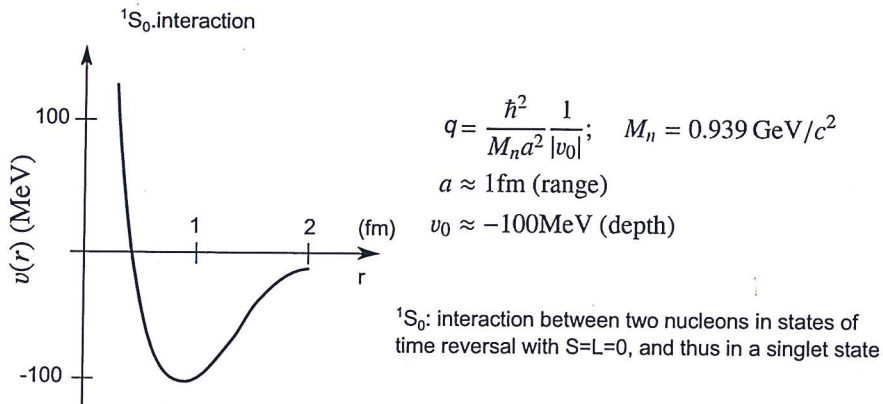
<sup>35</sup>Within this general context the physics embodied in the quantality parameter is closely related to that which is at the basis of the classical Lindemann criterion (Lindemann (1910)) to measure whether a system is ordered (e.g. a crystal) or disordered (e.g. a melted system) (Bilgram (1987), Löwen, H. (1994), Stillinger (1995)). The above statement is also true for the generalized Lindemann parameter (Stillinger and Stillinger (1990), Zhou et al. (1999)), used to provide similar insight into inhomogeneous finite systems like e.g. proteins (aperiodic crystals Schrödinger, E. (1944), see also Ehrenfest's theorem (Basdevant and Dalibard (2005) pag. 138)).

(1990)

constituents	$M/M_n$	$a(\text{cm})$	$v_0(\text{eV})$	$q$	phase( $T = 0$ )
${}^3\text{He}$	3	2.9(-8)	8.6(-4)	0.19	liquid <sup>a)</sup>
${}^4\text{He}$	4	2.9(-8)	8.6(-4)	0.14	liquid <sup>a)</sup>
$\text{H}_2$	2	3.3(-8)	32(-4)	0.06	solid <sup>b)</sup>
${}^{20}\text{Ne}$	20	3.1(-8)	31(-4)	0.007	solid <sup>b)</sup>
nucleons	1	9(-14)	100(+6)	0.4	liquid <sup>a),c),d)</sup>

✓ Table 2.3.1: Zero temperature phase for a number of systems<sup>a)</sup> a) delocalized (condensed), b) localized, c) non-Newtonian solid (cf. e.g. Bertsch (1988), de Gennes (1994), p. 25), that is, systems which react elastically to sudden solicitations and plastically under prolonged strain, d) paradigm of quantal, strongly fluctuating, finite many-body systems. While delocalization or less does not seem to depend much on whether one is dealing with fermions or bosons (Mottelson (1998) and refs. therein; cf also Ebran et al. (2014a), Ebran et al. (2014b), Ebran et al. (2013), Ebran et al. (2012)), the detailed properties of the corresponding single-particle motion are strongly dependent on the statistics obeyed by the associated particle (cf. Sect. 2.5).

next section



✓ (QM: ZPF ( $\Delta p_x \Delta x \geq \hbar$ ))

Figure 2.3.1: Schematic representation of the bare  $NN$ -interaction acting among nucleons displayed as a function of the relative coordinate  $r = |\mathbf{r}_1 - \mathbf{r}_2|$ , used to estimate the quantity parameter  $q$ , ratio of the zero point fluctuations (ZPF) of confinement and the potential energy.

of mass  $M$  ( $M_n$ : nucleon mass), the first four depending on atomic interactions (range  $A$ , strength  $meV$ ), the last one referring to the atomic nucleus.

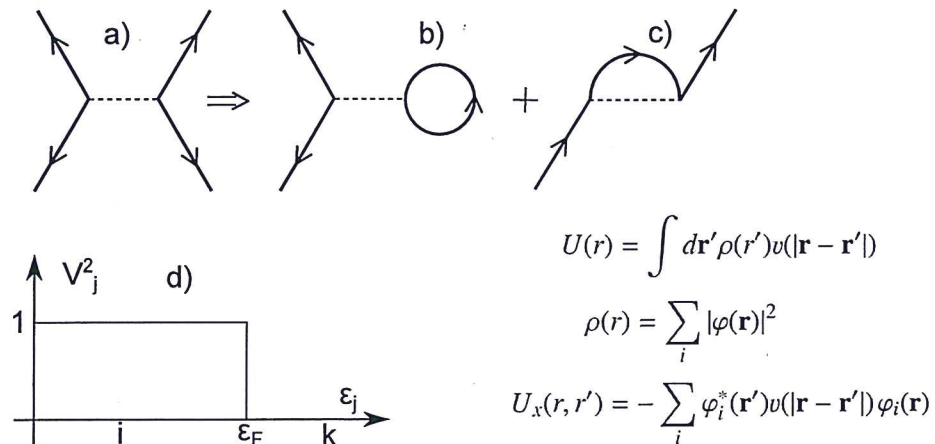


Figure 2.3.2: Schematic representation of (a) nucleon–nucleon scattering through the bare  $NN$ –interaction, (b) the associated contribution to the Hartree potential  $U(r)$  and, (c) to the Fock (exchange) potential  $U_x(r, r')$ ,  $\rho(r)$  being the nucleon density. (d) the Hartree–Fock solution leads to a sharp discontinuity at the Fermi energy  $\epsilon_F$ . That is, single-particle levels with energy  $\epsilon_i \leq \epsilon_F$  are fully occupied. Those with  $\epsilon_k \geq \epsilon_F$  empty.

### 2.4.1 independent-particle motion

In the previous section it was shown that the value of the quantity parameter associated with nuclei ( $q \approx 0.4$ ) leads to particle delocalization and likely makes the system amenable to a mean field description (Fig. 2.3.2; see however the provisos expressed at the end of Sect. 2.3). In such a case, Hartree–Fock approximation is tantamount to a selfconsistent relation between density and potential, weighted by the nucleon–nucleon interaction  $v$ , and leading to a complete separation between occupied ( $|i\rangle$ ) and empty ( $|k\rangle$ ) single-particle states,

$$(U_\nu^2 + V_\nu^2) = 1; \quad |\varphi_\nu\rangle = \bar{a}_\nu^\dagger |0\rangle = (U_\nu + V_\nu a_\nu^\dagger) |0\rangle; \quad V_\nu^2 = \begin{cases} 1 & \epsilon_i \leq \epsilon_F, \\ 0 & \epsilon_k > \epsilon_F. \end{cases} \quad (2.4.1)$$

The Hartree–Fock ground state can then be written as,

$$|HF\rangle = |\det(\varphi_\nu)\rangle = \Pi_\nu \bar{a}_\nu^\dagger |0\rangle = \Pi_i a_i^\dagger |0\rangle = \Pi_{i>0} a_i^\dagger a_{\tilde{i}}^\dagger |0\rangle. \quad (2.4.2)$$

where  $|\tilde{i}\rangle$  is the time reversed state to  $|i\rangle$ .

To be solved, the above self-consistent equations have to be given boundary conditions. In particular, make it explicit whether the system has a spherical or, for example, a quadrupole shape. That is, whether  $\langle HF | Q_2 | HF \rangle$  is zero or has a finite value,  $Q_{2M} = \sum_{j_1 j_2} \langle j_2 | r^2 Y_M^2 | j_1 \rangle [a_{j_1}^\dagger a_{j_2}]_M^2$  being the quadrupole operator which carries particle transfer quantum number  $\beta = 0$ , in keeping with its particle-hole character. In the case in which  $\langle Q_{2M} \rangle = 0$ , the system can display a spectrum of low-lying, large amplitude, collective quadrupole vibrations of frequency

$$\langle \gamma_2 || r^2 Y^2 || \gamma_1 \rangle$$

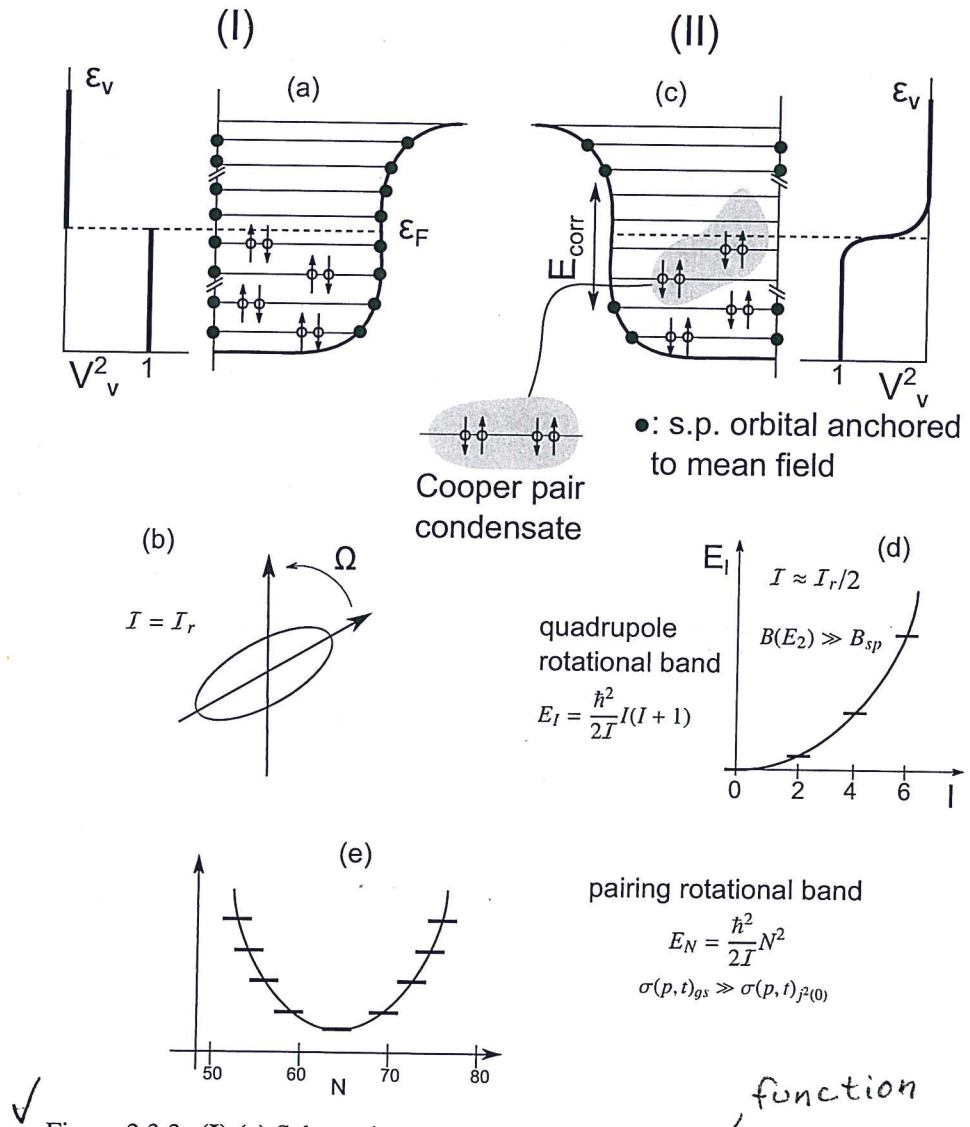


Figure 2.3.3: (I) (a) Schematic representation of “normal” (independent-particle) motion of nucleons in two-fold degenerate (Kramers, time-reversal degeneracy) orbits solidly anchored to the mean field and displaying a sharp, step-function-like, discontinuity in the occupancy at the Fermi energy lead to a deformed (Nilsson (1955)) rotating nucleus with a rigid moment of inertia  $I_r$  (b). (II) Schematic representation of independent nucleon Cooper pair motion in which few (of the order of 5-8) pairs lead to (c) a sigmoidal occupation transition at the Fermi energy and, having uncoupled themselves from the fermionic mean field being now (quasi) bosons they essentially do not contribute to (d) the moment of inertia of quadrupole rotational bands leading to  $I \approx I_r/2$  (cf. Belyaev, S. T. (2013), Belyaev (1959), Bohr, A. and Mottelson (1975) and references therein), (e) pairing rotational bands in gauge space, an example of which is provided by the ground states of the superfluid Sn-isotopes (see also Figs. 2.1.3 and 2.1.4).

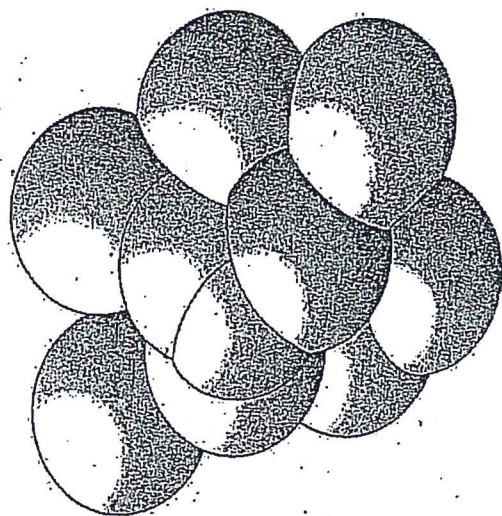
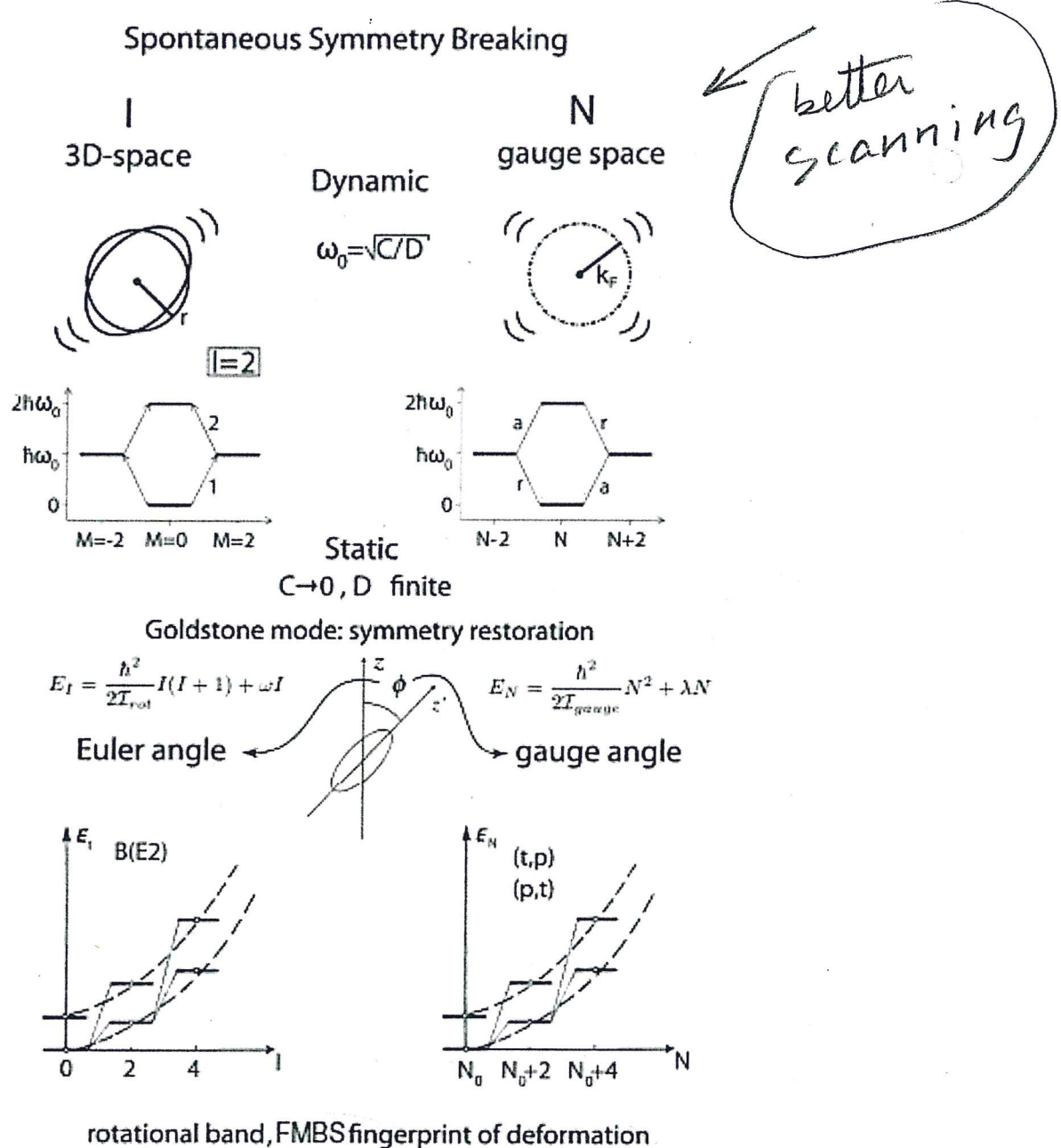


Figure 2.3.5: There are about  $10^{18}$  Cooper pairs per  $\text{cm}^3$  in a superconducting metal. A Cooper pair has a spatial extension of about  $10^{-4}$  cm. Thus a given Cooper pair will overlap with  $10^6$  other Cooper pairs, leading to strong pair-pair correlation, as schematically shown. This solution corresponds to the coherent solution of the many Cooper pair problem (coherent state), also valid in atomic nuclei (cf. Schrieffer (1964), Brink, D. and Broglia (2005), and references therein). (After Rogovin and Scully (1976)).

picture emerges from

solution of the superconducting state of metal



✓ Figure 2.4.1: Parallel between dynamic and static deformations in 3D- and in gauge-space for the nuclear finite many body system (FMBS). In the first case, the angular momentum  $I$  and the Euler angles are conjugate variables. In the second, particle number  $N$  and gauge angle. While the fingerprint of static (quadrupole and gauge) deformations are quadrupole and pairing rotational bands (see Fig. 2.1.4), vibrational bands are the expression of such phenomena in non deformed systems (after Broglia, R.A. et al. (1973)).